RESEARCH ARTICLE SCIENCE INTERNATIONAL

DOI: 10.17311/sciintl.2014.57.63

Similar Flow of Micropolar Fluids Between Two Disks in the Presence of a Magnetic Field

[1]Sajjad Hussain, [2]M. Anwar Kamal and [3]M. Shafique
[1]Centre for Advanced Studies in Pure and Applied Mathematics, B. Z. University, Multan, Pakistan
[2]Department of Mathematics, Suleman Bin Abdul Aziz University, Al-Kharj, Saudi Arabia
[3]Department of Mathematics, Gomal University, D. I. Khan, Pakistan

ABSTRACT

Background: The purpose of this study is to observe the effects of flow parameters on velocity and microrotation in a similar flow of micropolar fluids between two disks in the presence of a magnetic field. **Method:** In this analysis, the similarity transformations have been used to transform the governing highly non linear partial differential equations of motion. The resulting ordinary differential equations are solved numerically using Successive Over Relaxation (SOR) method and Simpson's (1/3) Rule. The numerical results have been improved by Richardson extrapolation to the limit. **Results:** The results have been obtained for velocity and microrotation for several values of the squeeze Reynolds number R and Hartmann number M and the material constants C's related to micropolar fluids viscosity coefficients. Comparison of the results for Newtonian and micropolar fluids is presented. **Conclusion:** The research concludes that the micropolar fluids flow resembles with that of Newtonian fluids when the material constants become close to zero but the micropolar behavior becomes prominent with the increasing values of these constants. The present results have practical applications in industry and lubrication phenomena.

Key words: Similar flow, micropolar fluids, numerical solution, magnetic field, reynolds number, richardson's extrapolation

Science International 2 (3): 57-63, 2014

INTRODUCTION

Eringen[1, 2] introduced and formulated the theory of micropolar fluids. These fluids exhibit certain microscopic effects due to the local structure and micro motions of the fluid elements. Ariman *et al*.[3] discussed special features of micropolar fluids. Moreover,[4,5] provided extensive surveys of literature of the theory of micropolar fluids .The flow of an electrically conducting fluid between two parallel, rotating disks in the presence of an external magnetic field is of interest in the study of certain geographical phenomena and also in the theory of magnetohyherodynamic (MHD) lubrication. The flow of fluid between parallel plates has attracted the attention of a lot of researchers. Singh and Smith[6] examined the plane parallel flow of micropolar fluids between two infinite plates with constant suction and injection. Kasiviswanathan and Gandhi[7] obtained a class of exact solutions for the MHD flow of a micropolar fluid confined between two infinite, insulated, parallel, non-coaxially rotating disks. Hussain and Kamal[8] studied boundary layer flow for micropolar electrically conducting fluid on a rotating disk in the presence of magnetic field. Unsteady flows of micropolar fluid have been considered by number of authors. Chawla[9] considered the micropolar fluid flow in the neighborhood of a flat plate started impulsively and found the dominant characteristics of two modes of wave propagation during the initial and final stages of growth. Pop[10] investigated the problem of unsteady flow past a wall which starts impulsively to stretch from rest. The motion of an electrically conducting fluid film squeezed between two parallel disks in the presence of a transverse magnetic field was studied by Hamza[11]. Flow of an electrically conducting non-Newtonian fluid past a stretching surface was studied by Able *et al*.[12] when a uniform magnetic field acts transverse to the surface. Hussain *et al*.[13] obtained numerical solutions for magnetohydrodynamic boundary layer flow over a rotating disk.

The present research deals with the study of similar flow of micropolar fluids between two parallel disks which at time t are spaced a distance $H(1-"t)^{1/2}$ apart and a magnetic field proportional to $B_0(1-"t)^{61/2}$ is applied perpendicular to the disks, where H denotes a representative length, B_0 denotes a representative magnetic field applied perpendicular to the disks and "G[1] denotes a representative time. The numerical results have been obtained for the velocity and micro rotation for different values of squeezing Reynolds number R in the range 0 < R#20 and the magnetic force parameter M in the range 0#M#50.

Corresponding Author: Sajjad Hussain, Centre for Advanced Studies in Pure and Applied Mathematics, B. Z. University, Multan, Pakistan

MATERIAL AND METHOD

The micropolar fluid flow is considered to be axisymmetric and incompressible. Fluid is contained between two parallel infinite disks. The distance between the disks at time t is h(t) = H(1-"t)$^{1/2}$. The upper disk is moving with velocity hr(t) towards the lower fixed disk. It is also supposed that the lower disk is at z = 0 and the upper one is at z = h(t), where h(0) = H. A magnetic field B(t) proportional to $B_0(1-"t)^{G1/2}$ is applied perpendicular to the two disks. The cylindrical coordinates (r, 2, z) are being used.

Under these assumptions the governing equations of motion for micropolar fluid are given as under:

$$\nabla.\underline{V} = 0 \tag{1}$$

$$-(\mu+\kappa)\nabla\times(\nabla\times\underline{V})+\kappa(\nabla\times\underline{\upsilon})-\nabla p+\underline{F}=\rho(\underline{V}.\nabla)\,\underline{V} \tag{2}$$

$$-\gamma\,(\nabla\times\nabla\times\underline{\upsilon})+\kappa(\nabla\times\underline{\mathbf{V}})-2\kappa\underline{\upsilon}=\rho\,j\,(\underline{\mathbf{V}}\,.\,\nabla)\,\underline{\upsilon} \tag{3}$$

Where x the velocity vector b, p the microrotation or spin, p the pressure, 0 the body force, D is the fluid density, μ denotes dynamic viscosity coefficient, j the micro-inertia density, (spin gradient density and 6 vortex density.

The electromagnetic body force as given by Rossow[14] is:

$$\underline{F}=\underline{J}\times\underline{B},\ \underline{J}\times\underline{B}=\underline{E}\sigma\,(\underline{V}\times\underline{B})\times\underline{B}=-\sigma\,B^2\,\underline{V} \tag{4}$$

Using the dimensional analysis, the velocity x(u, 0, w) and micro rotation 01(0, L2, 0) are assumed to be of the form:

$$u=\frac{\alpha r}{2(1-\alpha t)}f'(y),\ w=-\frac{\alpha H}{\sqrt{1-\alpha t}}f(y),\ \upsilon_2=\frac{\alpha r}{H(1-\alpha t)^{3/2}}L(y)$$
$$\text{where } y=\frac{z}{H\sqrt{1-\alpha t}} \text{ and } B=\frac{B_0}{\sqrt{1-\alpha t}} \tag{5}$$

The boundary conditions are as under:

$$u = 0,\ w = 0,\ L_2 = 0 \text{ at } z = 0$$

$$u = 0,\ w = hr,\ L_2 = 0 \text{ at } z = h(t)$$

The mass conservation Eq. 1 is identically satisfied and Eq. 2 yields:

$$\frac{1}{r}\frac{\partial P}{\partial r}=\frac{\rho\alpha^2}{4(1-\alpha t)^2}\left(\frac{1}{R}f'''-yf''-2f''-(f')^2+2ff''-M^2f'-2C_1L'\right) \tag{6}$$

$$\frac{\partial P}{\partial y}=\frac{-\rho\alpha^2H^2}{2(1-\alpha t)}\left\{\frac{1}{R}F''-yf'-f+2ff'-C_1L\right\} \tag{7}$$

Where:

$$R=\frac{\rho\alpha H^2}{2\mu} \text{ and } M^2=\frac{B_0{}^2\sigma}{\mu}$$

Whence the differentiation of Eq. 6 with respect y and Eq. 7 with respect to r lead to equation below after some manipulations:

$$R\{yf'''+3f''-2ff'''+2C_1L''\}+M^2f''=f'''' \tag{8}$$

and Eq. 3 yields:

$$2C_2L''+2f''L+C_3\,(f''-4L)=yL'+3L \tag{9}$$

where, prime denotes differentiation with respect to y and dimensionless material constants are given by:

$$C_1=\frac{\kappa}{\rho H^2\alpha},\ C_2=\frac{\gamma}{H^2\rho j\alpha} \text{ and } C_3=\frac{\kappa(1-\alpha t)}{\rho j\alpha}$$

The corresponding boundary conditions are:

$$f(0) = 0,\ fr(0) = 0,\ L(0) = 0$$
$$f(1) = 0.5,\ fr(1) = 0,\ L(1) = 0 \tag{10}$$

FINITE-DIFFERENCE EQUATIONS

For numerical purpose, equation (8) is integrated to yield:

$$R\{yf''+2f'-2f''+(f')^2+2C_1L'\}+M^2f'=f'''+c \tag{11}$$

where, C is a constant of integration. Now let:

$$fr = q \tag{12}$$

Equations 11 and 9, respectively become:

$$R\{yq'+2q-2fq'+(q)^2+2C_1L'\}+M^2q=q''+C \tag{13}$$

$$2C_2L''+2fL'-qL+C_3(q'-4L)=yL'+3L \tag{14}$$

subject to the boundary conditions:

$$f(0) = 0,\ q(0) = 0,\ L(0) = 0$$
$$f(1) = 0.5,\ q(1) = 0,\ L(1) = 0 \tag{15}$$

In order to obtain the numerical solution of nonlinear ordinary differential Eq. 13 and 14, these equations are approximated by using central difference approximation at a typical point $y = y_n$ of the interval (0, 1) and yield respectively:

$$(1-Rh(\frac{y}{2}-fn))q_{n+1}-(2+h^2M^2+h^2R(2+q_n))q_n +(1+Rh(\frac{y}{2}-fn))q_{n-1}-C_1h(L_{n+1}-L_{n-1})+h^2\beta=0 \quad (16)$$

$$(2C_2-h(\frac{y}{2}-f_n))L_{n+1}-(4C_2+4C_3h^2+3h^2+h^2q_n)L_n +(2C^2+h(\frac{y}{2}-f_n))L_{n-1}+C_3\frac{h}{2}(q_{n+1}-q_{n-1})=0 \quad (17)$$

where, h denotes a grid size. The Eq. 12 is integrated numerically. Also the symbols used denote $q_n = q(y_n)$, $f_n = f(y_n)$ and $L_n = L(y_n)$

COMPUTATIONAL PROCEDURE

Finite difference equations 16 and 17 and the first order ordinary differential equations 12 are solved simultaneously by using SOR method Smith[15] and Simpson's (1/3) rule Gerald[16] with the formula given in Milne[17], respectively subject to the appropriate boundary conditions.

The order of the sequence of iterations is as follows:

- The equations (16) and (17) for the solution of *q* and L are solved subject to the following boundary conditions:

$$q = 0, L = 0 \text{ at } y = 0$$
$$q = 0, L = 0 \text{ at } y = 1$$

- For the solution of f, the computed values of q from above step are used in to equations (12) and then integrated by Simpson's (1/3) rule subject to the following initial conditions:

$$f = 0 \qquad \text{at } y = 0$$

- The optimum value of the relaxation parameter τ_{opt} is estimated to accelerate the convergence of the SOR method
- The SOR procedure is terminated when the following criterion is satisfied for each of q and L:

$$\max_{i=1}^{n}\left|U_i^{n+1}-U_i^n\right|<10^{-6}$$

where, n denotes the number of iterations and U stands for each of q and L.

The above steps 1 to 4 are repeated for higher grid levels h/2 and h/4. The SOR procedure gives the solution of f and L of order of accuracy $O(h^2)$due to second order finite differences used in Eq. 16 and 17. While Simpson's (1/3) rule gives the order of accuracy $O(h^5)$in the solution of f. Higher order accuracy of $O(h^6)$ in the solution of f on the basis of above solution is achieved by using Richardson's extrapolation to the limit Burden[18]. The constant of integration C is determined by hit and trial using the zero-order perturbation results $f = y^2 (3/2-y)$, $f = 3y(1-y)$ in the region of mid plane $y = 1/2$.

RESULTS AND DISCUSSION

The numerical results for velocity components f, f and microrotation function L have been computed for different values of R and M for three different sets of material constants C_1, C_2 and C_3, chosen arbitrarily and given in the Table 1.

The accuracy of numerical results is checked by comparing the results on different grid sizes, namely h = 0.025, 0.0125 and 0.006. The different cases of the material constants as given in Table 1 have been considered. It is observed that the micropolarity of the fluids becomes more prominent for larger values of these constants than the smaller values. Also, the numerical results have been obtained separately for three different cases of these constant to make a better understanding of the behavior of micropolar fluids. The results of f, f and L are given in Table 2 and 3 in the case-II of material constants. The extrapolated results for f' are given in the Table 4 and 5 in the case-III of material constants. The comparison for Newtonian and micropolar fluids is given in Table 6.

Graphically, Fig. 1a shows the radial velocity f for small R and large values of M. Fig. 1b-c exhibit the pattern of radial flow f' for small values of R with slight and moderate magnetic field M. Fig. 1d depicts the radial velocity distribution for moderate squeezing Reynolds number R with small values of M .The results for large squeezing and small to medium values of M is presented in Fig. 1e-f. The comparison of Newtonian fluid and micropolar fluid flow is given in the Fig. 2a-b. Figures 3a-c demonstrate the non- dimensional microrotation field L for different values of the

Table 1: Three different sets of material constants C_1, C_2 and C_3

Cases	C_1	C_2	C_3
I	0.1	0.05	0.01
II	1.0	0.50	0.10
III	0.5	1.50	2.50

Table 2: Numerical results of f, fN and L using SOR method and Simpson's Rule on finer grid size for specified values of the parameters R, M and the case-II of material constants

M = 10.0, R = 0.01				M = 40.0, R = 0.01			
y	f	fN	L	y	f	fN	L
0.000	0.000000	0.000000	0.000000	0.000	0.000000	0.000000	0.000000
0.200	0.070936	0.540262	0.002260	0.200	0.092088	0.526217	0.000330
0.400	0.188513	0.612169	0.000493	0.400	0.197363	0.526392	-0.000364
0.600	0.311567	0.612156	-0.001446	0.600	0.302641	0.526391	-0.000761
0.800	0.429140	0.540227	-0.002884	0.800	0.407914	0.526210	-0.001007
1.000	0.500070	0.000000	0.000000	1.000	0.500002	0.000000	0.000000

Table 3: Numerical results of f, f' and L using SOR method and Simpson's Rule on finer grid size for specified values of the parameters R, M and the case-II of material constants

M = 5.0, R = 15.0				M = 10.0, R = 20.0			
y	f	fN	L	y	f	fN	L
0.000	0.000000	0.000000	0.000000	0.000	0.000000	0.000000	0.000000
0.200	0.066310	0.529209	0.002777	0.200	0.074663	0.545288	0.001934
0.400	0.185596	0.634660	0.000878	0.400	0.190311	0.593132	0.000348
0.600	0.313725	0.635368	-0.001550	0.600	0.309257	0.593313	-0.001230
0.800	0.433321	0.531648	-0.003219	0.800	0.425026	0.546556	-0.002501
1.000	0.500083	0.000000	0.000000	1.000	0.500035	0.000000	0.000000

Table 4: Numerical results using Richardson extrapolation method for fN for specified values of the parameters R, M and the case-III of material constants

M = 0.0, R = 0.01					M = 30.0, R = 0.01				
h = 0.025	h = 0.012	h = 0.006	Extrapolated		h = 0.025	h = 0.012	h = 0.006	Extrapolated	
y	fN	fN	fN	fN	y	fN	fN	fN	fN
0.000	0.000000	0.000000	0.000000	0.000000	0.000	0.000000	0.000000	0.000000	0.000000
0.200	0.484843	0.484875	0.484914	0.484929	0.200	0.534317	0.534454	0.534494	0.534508
0.400	0.730746	0.730789	0.730845	0.730867	0.400	0.535788	0.535799	0.535806	0.535809
0.600	0.730762	0.730797	0.730851	0.730873	0.600	0.535770	0.535780	0.535815	0.535830
0.800	0.484872	0.484890	0.484925	0.484939	0.800	0.534267	0.534405	0.534439	0.534450
1.000	0.000000	0.000000	0.000000	0.000000	1.000	0.000000	0.000000	0.000000	0.000000

Table 5: Numerical results using Richardson extrapolation method for f' for specified values of the parameters *R*, M and the case-III of material constants

M = 0.0, R = 20.0					M = 20.0, R = 20.0				
h = 0.025	h = 0.012	h = 0.006	Extrapolated		h = 0.025	h = 0.012	h = 0.006	Extrapolated	
y	f'	f'	f'	f'	y	f'	f'	f'	f'
0.000	0.000000	0.000000	0.000000	0.000000	0.000	0.000000	0.000000	0.000000	0.000000
0.200	0.516654	0.521238	0.523252	0.524000	0.200	0.542790	0.544709	0.545498	0.545789
0.400	0.642731	0.644459	0.645125	0.645369	0.400	0.593001	0.593513	0.593532	0.593529
0.600	0.648032	0.646969	0.646376	0.646149	0.600	0.593802	0.593615	0.593559	0.593540
0.800	0.532886	0.528995	0.527106	0.526395	0.800	0.548142	0.547132	0.546586	0.546378
1.000	0.000000	0.000000	0.000000	0.000000	1.000	0.000000	0.000000	0.000000	0.000000

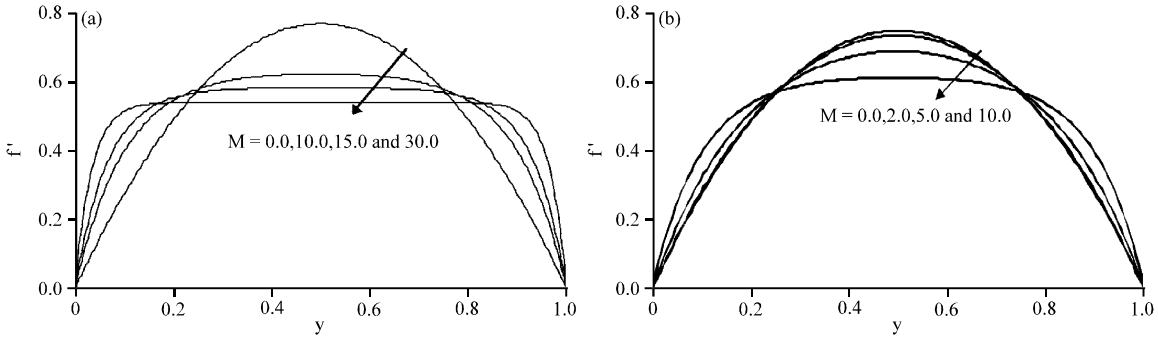

Fig. 1: Continue

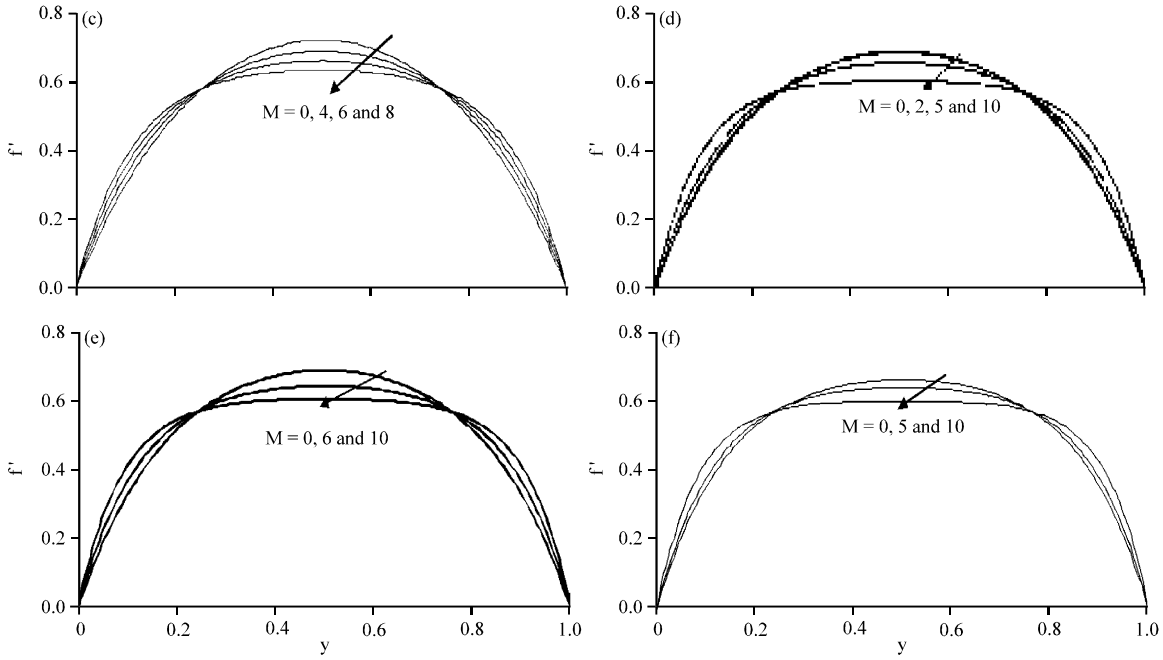

Fig. 1(a-f): (a) Graph of f' for different values of M when R = 0.01 and the case-II of material constants, (b) Graph of f' for different values of M when R = 1.0 and the case-II of material constants, (c) Graph of f' for different values of M when R = 5.0 and the case-II of material constants, (d) Graph of' for different values of M when R = 10.0 and the case-II of material constants, (e) Graph of ' for different values of M when R = 15.0 and the case-II of material constants and (f) Graph of f' for different values of M when R = 20.0 and the case-II of material constants . Graph of f' for different values of M when (a) R = 0.01 (b) R = 1.0 (c) R = 5.0, (d) R = 10.0 (e) R = 15.0 (f) R = 20.0 and the case-II of material constants

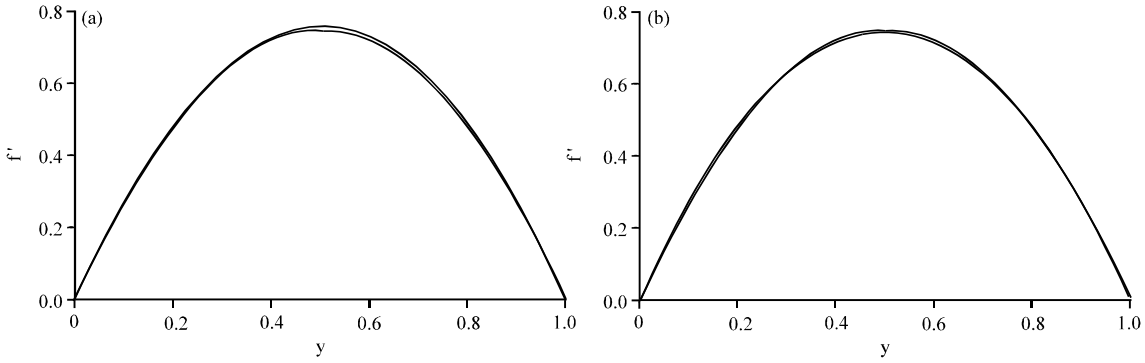

Fig. 2(a-b): (a) Comparison of f' for micropolar and Newtonian fluids from top to bottom for the values of R = 0.01, M = 0.0 and the case-III of material constants and (b) Comparison of f' for micropolar and Newtonian fluids from top to bottom for the values of R = 1.0, M = 0.0 and the case-III of material constants. Comparison of f' for micropolar and Newtonian fluids from top to bottom for the values of (a) R = 0.01, M = 0.0 (b) R = 1.0, M = 0.0 and the case-III of material constants

parameters R and M. The magnitude of microrotation decreases with increasing values of M and increasing values of Reynold's number R decrease the microrotation.

Usual parabolic distribution in the radial direction is observed. Further, it is found that for fixed R, there is a slight increase in the value of f' near the disks and a slight decrease in the region of the mid plane with

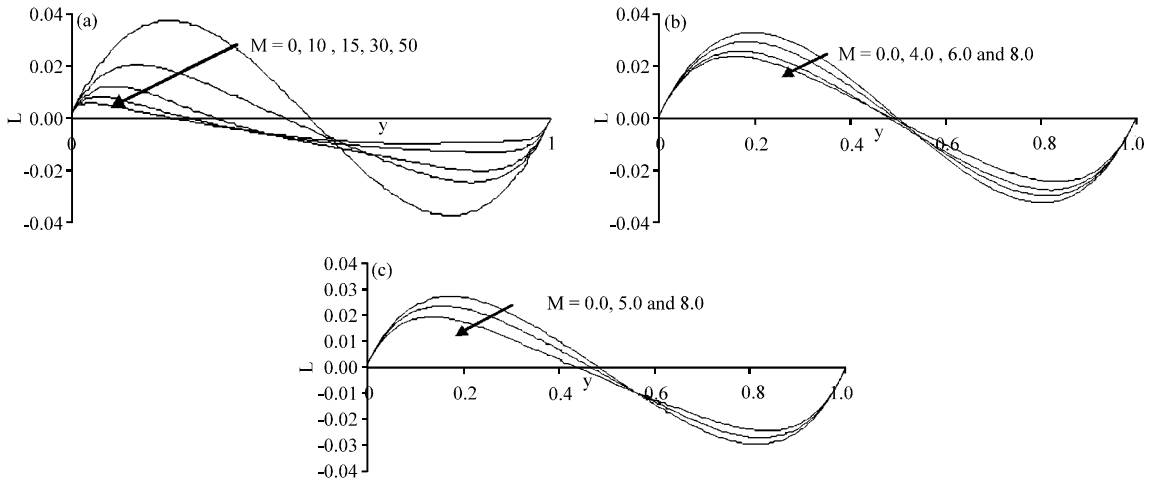

Fig. 3(a-c): (a) Graph of non dimensional microrotation component L for R = 0.0, for different values of M and the case-II of material constants, (b) Graph of non dimensional microrotation component L for R = 5.0, for small and moderate values of M and the case-II of material constants and (c) Graph of non dimensional microrotation component L for large squeezing. Reynolds number R = 15.0, for small and moderate values of M and the case-II of material constants. Graph of non dimensional microrotation component L for (a) R = 0.0, for different values of M (b) for R = 5.0, for small and moderate values of M (c) for large squeezing Reynolds number R = 15.0, for small and moderate values of M and the case-II of material constants

increase in the values of M. This increase and decrease become more prominent with more increase in M, also the radial velocity profiles become more flat in the interior region for all values of R. While the magnitude of radial flow decreases with increase in R for fixed values of M. These results agree with the previous findings as given by Hamza[19], Hussain[20].

CONCLUSION

The similar flow of micropolar fluids between two disks in the presence of a magnetic field is considered. The value velocity component f' is larger for micropolar fluids than for Newtonian fluids. The increasing magnitude of the magnetic field decreases the microrotation. Also, the increasing values of Reynold number R decrease the microrotation. The material constants C's affect the microrotation of micropolar fluids flow. If one of these constants C_1 is zero the micropolar fluid flow becomes the Newtonian fluid flow.

REFERENCES

1. Eringen, A.C., 1964. Simple microfluids. Int. J. Eng., 2: 205-217.
2. Eringen, A.C., 1966. Theory of micropolar fluids. J. Math. Mech., 16: 1-18.
3. Ariman, T., M.A. Turk and N.D. Sylvester, 1973. Microcontinuum fluid mechanics: A review. Int. J. Eng. Sci., 11: 905-930.
4. Lukaszewicz, G., 1999. Micropolar Fluids: Theory and Application. Birkhauser, Basle, Switzerland, ISBN-13: 9780817640088, Pages: 253.
5. Eringen, A.C., 2001. Microcontinuum Field Theories II Fluent Media. 1st Edn., Springer, New York, USA., ISBN-13: 978-0387989693, Pages: 356.
6. Singh, G. and A.C. Smith, 1973. Flows of micropolar fluid suction and injection. Tensor, N.S., 27: 131-134.
7. Kasiviswanathan, S.R. and M.V. Gandhi, 1992. A class of exact solutions for the magnetohydrodynamic flow of a micropolar fluid. Int. J. Eng. Sci., 30: 409-417.
8. Hussain, S. and M.A. Kamal, 2012. Magnetohydrodynamic boundary layer micropolar fluid flow over a rotating disk. Int. J. Comput. Applied Math., 7: 301-313.
9. Chawla, S.S., 1972. Boundary layer growth of a micropolar fluid. Int. J. Eng. Sci., 10: 981-987.
10. Pop, I., 1996. Unsteady flow past a stretching sheet. Mech. Res. Commun., 23: 413-422.
11. Hamza, E.A., 1992. Unsteady flow between two disks with heat transfer in the presence of a magnetic field. J. Phys. D: Applied Phys., 25: 1425-1431.
12. Able, S., P.H. Veena, K. Rajgopal and V.K. Pravin, 2004. Non-Newtonian magnetohydrodynamic flow over a stretching surface with heat and mass transfer. Int. J. Non-Linear Mech., 39: 1067-1078.

13. Hussain, S., M.A. Kamal, F. Ahmad, M. Shafique and M. Ali, 2013. Numerical solution for newtonian maganatohydrodynamic boundary layer flow over a rotating disk. Int. J. Applied Math. Mech., 2: 1-10.
14. Rossow, V.J., 1958. On flow of electrically conducting fluids over a flat plate in the presence of a transverse magnetic field. NASA-Report-1358. http://naca.central.cranfield.ac.uk/reports/1958/naca-report-1358.pdf.
15. Smith, G.D., 1979. Numerical Solution of Partial Differential Equations: Finite Difference Methods. Clarendon Press, Oxford, UK.
16. Gerald, C.F. and P.O. Wheatley, 1989. Applied Numerical Analysis. Addison-Wesley Publ., New York, USA., Pages: 722.
17. Milne, W.E., 1970. Numerical Solution of Differential Equation. Dover Publ., USA., ISBN-13: 978-0486624372, Pages: 359.
18. Burden, R.I., 1985. Numerical Analysis. 3rd Edn., Prindle, Weber and Schmidt, Boston, USA.
19. Hamza, E.A., 1987. A similar flow between two disks in the presence of a magnetic field. International Centre for Theoretical Physics Series No. 87/287, Trieste, Italy.
20. Hussain, S., M.A. Kamal, F. Ahmad, M. Ali, M. Shafique and S. Hussain, 2013. Numerical solution for a similar flow between two disks in the presence of a magnetic field. Applied Math., 4: 1163-1167.